High-order effects in Rayleigh-type optical mixing

F. García-Golding and A. Marcano O.
Instituto Venezolano de Investigaciones Científicas, Centro de Física, Apartado Postal 1827, Caracas 1010A, Venezuela
(Received 11 September 1984; revised manuscript received 11 February 1985)

A nonperturbative analysis (in one of the fields) of the Rayleigh-type optical-mixing signal in an absorbing medium shows that it is more sensible to saturation than the effect that could be expected from "absorption saturation arguments." We also report the observation of such high-order effects in the organic dye malachite green. We have found that an effective two-level system model with a longitudinal relaxation time of 1.1 ± 0.2 ps, a transverse relaxation time of 0.13 ± 0.05 ps, and a transition moment of 1.2 D account for the deviation from the third-order regime. However, the frequency region of the data that follows the predicted spectral deformation is power dependent and it shrinks as power increases.

I. INTRODUCTION

The use of two optical fields $\mathbf{E}_1$ and $\mathbf{E}_2$ of frequencies ω_1 and ω_2 to induce population oscillations at the frequency $\Delta\omega=\omega_1-\omega_2$ in a material medium and the simultaneous observation of the scattering of these fields (or another field) has been very powerful for the determination of the longitudinal relaxation time T_1 and/or the transverse relaxation time T_2. Frequency-domain experiments as Rayleigh-type optical[1-3] mixing (RTOM), polarization spectroscopy (PS),[4,5] and the three-laser-grating technique[6,7] (TLG) of Siegman fall within this category.

In a PS experiment the phase-memory information (T_2) is extracted from hole-burning effects rather than from population oscillation. The TLG technique of Siegman is not expected to be sensible for the determination of T_2. Recently, time-domain techniques as two-pulse[8] scattering (self-diffraction) and three-pulse[9] scattering (transient-induced grating) have been demonstrated to be sensible to T_2.

The lowest-order nonlinear response involved in this experiment is the third-order susceptibility; however, sometimes the experimental situation is such that it is not possible to stay within this perturbation order. Therefore it is important to examine first, how important are the next terms in the perturbation expansion, and second, how to extract more information from these high-order effects.

In this paper we show, using a nonperturbative treatment that the RTOM signal at $\omega_3=2\omega_1-\omega_2$ saturates at power levels significantly lower than those expected from the simple saturation absorption arguments. We also report the first observation of this high-order effect in malachite green and use it to estimate the transition moment.

II. THEORY

Let us consider two incident light waves of frequencies ω_1 and ω_2 nearly resonant with a transition ($a\rightarrow b$) assumed inhomogeneously broadened. The density-matrix equations describing this system are

$$\frac{d\rho_D}{dt}=-\frac{2i}{\hbar}(H_{ab}\rho_{ba}-\rho_{ab}H_{ba})-\frac{1}{T_1}[\rho_D-\rho_D^{(0)}]\,, \tag{1}$$

$$\frac{d\rho_{ba}}{dt}=-\frac{i}{\hbar}H_{ba}\rho_D-\left[\frac{1}{T_2}+i\omega_0\right]\rho_{ba}\,, \tag{2}$$

$$H_{ba}=(-\boldsymbol{\mu}_{ba}\cdot\mathbf{E}_1e^{-i\omega_1t}-\boldsymbol{\mu}_{ba}\cdot\mathbf{E}_2e^{-i\omega_2t})+\text{c.c.}\,, \tag{3}$$

where $\rho_D=\rho_{aa}-\rho_{bb}$, the superscript (0) denotes equilibrium value, $\boldsymbol{\mu}_{ba}$ is the electric transition moment, $\mathbf{E}_1$ and $\mathbf{E}_2$ are the electric field amplitudes of the light waves, and ω_0 is the resonant frequency of the transition.

In order to obtain $\rho_{ba}(\omega_3)$ we solve the above equations simultaneously for $\rho_{ba}(\omega_2)$, $\rho_D(\omega_2-\omega_1)$, $\rho_{ab}(\omega_2-2\omega_1)$, and $\rho_{ab}(-\omega_1)$ after finding the zeroth-order solution in E_2. The only restriction is that we keep E_2 at first order. In this way we obtain the following relations:

$$D_2\rho_{ba}(\omega_2)=\frac{i}{\hbar}\boldsymbol{\mu}_{ba}\cdot\mathbf{E}_2\rho_D^{\text{dc}}+\frac{i}{\hbar}\boldsymbol{\mu}_{ba}\cdot\mathbf{E}_1\rho_D(\omega_2-\omega_1)\,, \tag{4}$$

$$\begin{aligned}\Gamma_1(\Delta)\rho_D(\omega_2-\omega_1)=&\frac{2i}{\hbar}\boldsymbol{\mu}_{ab}\cdot\mathbf{E}_1^*\rho_{ba}(\omega_2)\\&-\frac{2i}{\hbar}\boldsymbol{\mu}_{ba}\cdot\mathbf{E}_1\rho_{ab}(-\omega_3)\\&-\frac{2i}{\hbar}\boldsymbol{\mu}_{ba}\cdot\mathbf{E}_2\rho_{ab}(-\omega_1)\,,\end{aligned} \tag{5}$$

$$D_3^*\rho_{ab}(-\omega_3)=-\frac{i}{\hbar}\boldsymbol{\mu}_{ab}\cdot\mathbf{E}_1^*\rho_D(\omega_2-\omega_1)\,, \tag{6}$$

and

$$D_1^*\rho_{ab}(-\omega_1)=-\frac{i}{\hbar}\boldsymbol{\mu}_{ab}\cdot\mathbf{E}_1^*\rho_D^{\text{dc}}\,, \tag{7}$$

where

$$D_j=\frac{1}{T_2}+i(\omega_0-\omega_j),\quad j=1,2,3$$

$$\Gamma_1(\Delta)=\frac{1}{T_1}+i(\omega_2-\omega_1),\quad \Delta=\omega_2-\omega_1$$

and

$$\rho_D^{\rm dc}=\rho_D^{(0)}\left[1+\frac{4\Omega^2T_1}{|D_1|^2T_2}\right]^{-1},\quad \Omega^2=\frac{|\mu_{ba}\cdot\mathbf{E}_1|^2}{\hbar^2}.$$

The solution for $\rho_{ab}(\omega_3)$ is

$$\rho_{ba}(\omega_3)=\rho_{ba}^{(3)}(\omega_3)F(S)\,, \tag{8}$$

where

$$F(S)=\left[\frac{|D_1|^2T_2^2}{|D_1|^2T_2^2+4S}\right]\times\left[\frac{\Gamma_1^*(\Delta)D_3D_2^*T_1T_2^2}{[\Gamma_1^*(\Delta)D_3D_2^*T_1T_2^2+4S(1+i\Delta T_2)]}\right], \tag{9}$$

$$\rho_{ba}^{(3)}(\omega_3)=-\left[\frac{2i}{\hbar^3}\right]\left[\frac{(\mu_{ba}\cdot\mathbf{E}_1)^2(\mu_{ab}\cdot\mathbf{E}_2^*)}{\Gamma_1^*(\Delta)D_3}\right]\times\left[\frac{1}{D_2^*}+\frac{1}{D_1}\right][\rho_D^{(0)}\exp(-i\omega_3t)]\,, \tag{10}$$

$$S=\frac{I}{I_s},\quad I=\frac{c}{2\pi}|\mathbf{E}_1|^2,\quad\text{and}\quad I_s=\frac{\hbar^2c}{2\pi|\mu_{ba}|^2T_1T_2}\,. \tag{11}$$

The component $\rho_{ba}^{(3)}(\omega_3)$ is the lowest-order solution previously reported.[2] The signal is proportional to the square modulus of the complex polarization

$$\mathbf{P}=N\int_{-\infty}^{\infty}\langle\rho_{ba}\mu_{ab}\rangle g(\omega_0)d\omega_0\,, \tag{12}$$

where N is the density of the absorbing species, the angular brackets denote an ensemble average over the initially isotropic orientational distribution, and $g(\omega_0)$ is the distribution of resonant frequencies ω_0. We will introduce the following approximation for the complex polarization:

$$\mathbf{P}\cong N\int_{-\infty}^{\infty}\langle\rho_{ba}^{(3)}\mu_{ab}\rangle F(S)g(\omega_0)d\omega_0\,, \tag{13}$$

where

$$S=\frac{I}{I_s}\quad\text{and}\quad I_s=\frac{\hbar^2c}{2\pi\langle|\mu_{ba}|^2\rangle T_1T_2}\,. \tag{14}$$

The right-hand side of Eq. (13) is the scalar contribution to the nonlinear polarization. Also, let us work with the same polarization for the signal pump and probe fields, and write the scalar equation

$$P=\chi_{\rm eff}E_1^2E_2^*\exp(-i\omega_3t)\,, \tag{15}$$

where $\chi_{\rm eff}$ is an intensity-dependent effective nonlinear susceptibility.

The high-order contribution to $\chi_{\rm eff}$ is contained in the function $F(S)$. It has two saturation factors which could be named as dc and ac saturation factors. The dc saturation factor accounts for the dc change of the population at all order in the pump field, and is well known in absorption saturation experiments. The ac saturation factor accounts the feature of the ac component of the population change.

It turns out that the fifth-order contribution to the signal at $\omega_3=2\omega_1-\omega_2$ arriving from the second-order expansion of the ac saturation factor are the same as those found by Yajima *et al.*[2] The high sensibility of the RTOM signal to saturation effects can be seen if we consider the limiting case $|\Delta|\ll 1/T_1,\ 1/T_2$ in Eqs. (9) and (10). In this case we have that

$$D_j\cong D_1,\quad j=1,2,3$$

$$\Gamma_1(\Delta)\cong\frac{1}{T_1},\quad F(S)\cong\left[\frac{|D_1|^2T_2^2}{|D_1|^2T_2^2+4S}\right],$$

and

$$\rho_{ba}^{(3)}(\omega_3)\propto\frac{T_1}{T_2}\frac{E_1^2E_2^*}{D_1|D_1|^2}\exp(-i\omega_3t)\,.$$

Introducing this approximate expression in Eq. (8) we obtain

$$\rho_{ba}(\omega_3)\propto\frac{D_1T_2^3T_1}{(|D_1|^2T_2+4S)^2}E_1^2E_2^*\exp(-i\omega_3t)\,.$$

From this equation and Eqs. (12), (13), and (15) it follows that the effective susceptibility is

$$\chi_{\rm eff}\propto\int_{-\infty}^{\infty}\frac{g(\omega_0)D_1}{(|D_1|^2T_2^2+4S)^2}d\omega_0\,. \tag{16}$$

If the inhomogeneous width $(\Delta\omega)_i$ is broad enough to satisfy the condition

$$(\Delta\omega_i)\gg T_2^{-1},\ T_1^{-1}\,,$$

the integration of Eq. (16) can be carried out by taking $g(\omega_0)$ out of the integral, leading to

$$\chi_{\rm eff}\propto\frac{1}{(1+4S)^{3/2}},\quad|\chi_{\rm eff}|^2\propto\frac{1}{(1+4S)^3}\,. \tag{17}$$

Note that this power dependence is stronger than the well-known $(1+4S)^{-1/2}$ power dependence for the absorption of the pump beam. Therefore, our saturation effect will be observable at significantly lower values of S than in the case of saturation of the absorption in hole-burning experiments.

III. EXPERIMENTAL RESULTS

In order to observe the above-mentioned high-order effect we choose the organic dye malachite green on which small absorption saturation effects have been qualitatively reported by Trebino *et al.*[7] Organic dyes are not simple systems. It has been learned from hole-burning[8] and optical mixing experiments[3] that spectral diffusion is always present in these systems. The contribution of these effects to the RTOM signal is expected in the low-frequency region $\omega_1-\omega_2\lesssim 1/T_2$. Also, contributions from the presence of additional levels are expected in the same region.

We use two dye lasers (Molectron DL200) pumped by a N_2 laser (Molectron UV1000). The pump beam (ω_1) has $\sim$360-μJ pulses of 610-nm wavelength with a repetition rate of 15 pulses per second. The pulses are approximately 6 ns in length and have a spectral linewidth of 0.4 ± 0.2 cm^{-1}. The probe beam (ω_2) was about 20 times weaker than the pump beam. The two beams overlap inside a glass sample cell (0.25-mm internal width; Wilmad Glass

Company, Inc.) focused by a 20-cm lens. The intensity of the pump beam is accurately set by a continuous variable attenuator. Pulses energy were measured with a LP141 Molectron detector. The polarization was the same for the signal, the pump, and the probe. The signal was collected with a 0.5-cm^{-1} resolution Jobin Yvon Ramanor H625 spectrometer and a photomultiplier in conjunction with a Molectron LP20 boxcar. The estimated spot size of the beams in the sample cell is about 20 μm in diameter. We used samples of 5×10^{-4}-M/l solution of malachite green in water.

Figure 1 shows the intensity dependence of $|\chi_{\text{eff}}|^2$ for $\Delta=5$, 15, and 20 cm^{-1} and Fig. 2 shows the frequency dependence of $|\chi_{\text{eff}}|^2$ for $S=0.03$.

It should be noted that in Fig. 1 different curves have been properly shifted vertically with respect to each other for easy observation and therefore relative magnitudes for different curves are meaningless. The solid line for $\Delta=5$ cm^{-1} was drawn using Eq. (15) after numerical integration with a inhomogeneous Gaussian distribution for $g(\omega_0)$ of linewidth 800 cm^{-1} half-width at half maximum (HWHM), with $T_1=1.1\pm0.2$ ps, $T_2=0.13\pm0.05$ ps, and $I_s=1.5\times10^9$ W/cm^2. Except for a vertical scale factor, the prediction for $\Delta=15$ cm^{-1} with the above parameters is also drawn. The deviation from the third-order prediction appears in Fig. 1 as the curvature of the function $|\chi_{\text{eff}}|^2$ versus S. In order to find T_1, T_2, and I_s in Figs. 1 and 2, and S in Fig. 2, the following procedure was carried out:

(a) The frequency spectra at low intensity (Fig. 2) was used to determine initial values for T_1 and T_2.

(b) Using the above values the final fitting was done with the data of Fig. 1 at $\Delta=5$ cm^{-1}. This gave final values for T_2 and I_s. From this, the saturation parameter S for Fig. 1 was deduced.

From the parameters T_1, T_s, I_s, and S for given intensity, and using Eq. (14) we get $1.2D$ for the transition moment. On the other hand, absorption measurements in the same sample yield a value of $3D$. The first value is critically dependent on the estimated spotsize of the beam in the sample cell, however in spite of this the agreement is reasonable. Existence of this difference in the calculated dipole moments will be discussed below.

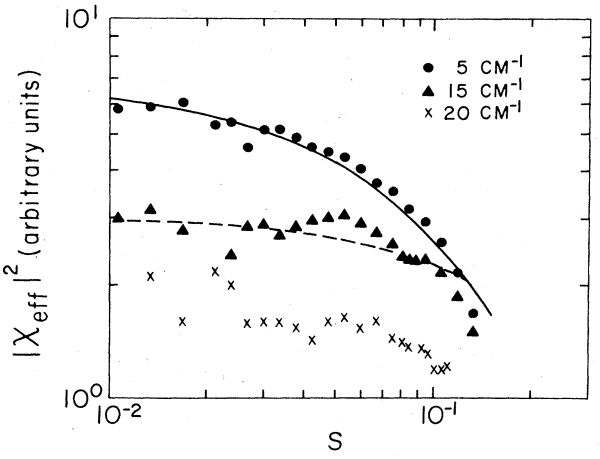

FIG. 1. $|\chi_{\text{eff}}|^2$ vs normalized intensity $S=I/I_s$. The solid line for $\Delta=5$ cm^{-1} was drawn using Eq. (15) with $T_1=1.1\pm0.2$ ps, $T_2=0.13+0.05$ ps, $I_s=1.5\times10^9$ W/cm^2, and an inhomogeneous linewidth of 800 cm^{-1} (HWHM). Except for a vertical scale factor the prediction for $\Delta=15$ cm^{-1} with the above parameters is also drawn (dashed line).

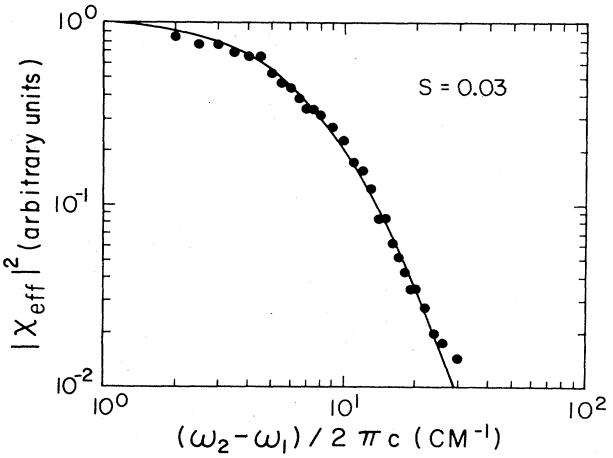

FIG. 2. Frequency dependence of $|\chi_{\text{eff}}|^2$ for $S=0.03$ (solid line) was drawn using Eq. (15) with T_1, T_2, I_s, and the inhomogeneous linewidth as used in Fig. 1.

Figures 3 and 4 show the frequency dependence on $|\chi_{\text{eff}}|^2$ for $S=0.06$ and 0.13, respectively. T_1 and T_2 are the same as used in Fig. 2. The broadening effect for intensities $\sim10^8$ W/cm^2, $S=0.06$ is reasonably predicted for this model, but the departures from the prediction at intensities twice larger 2×10^8 W/cm^2, $S=0.13$ becomes notable. Such deviations could be the result of neglecting spectral diffusion.

There have been several reports on the population relaxation times in malachite green in different solvents. The relaxation times for low-viscosity solvents are shown in Table I. Also, PS experiments[4] on the same material estimate the transverse relaxation time T_2 in less than 0.02 ps.

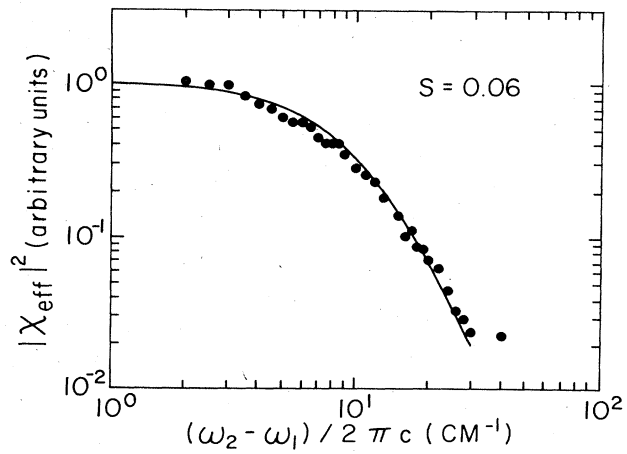

FIG. 3. Frequency dependence of $|\chi_{\text{eff}}|^2$ for $S=0.06$ (solid line) was drawn using Eq. (15) with T_1, T_2, I_s, and the inhomogeneous linewidth as used in Fig. 1.

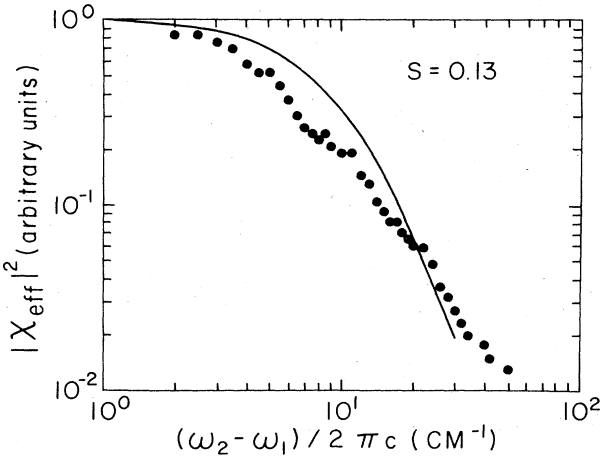

FIG. 4. Frequency dependence of $|\chi_{\text{eff}}|^2$ for $S=0.13$ (solid line) was drawn using Eq. (15) with T_1, T_2, I_s, and the inhomogeneous linewidth as used in Fig. 1.

Our population relaxation time of 1.1 ± 0.2 ps is in good agreement with the values shown in Table I. However, in view of the multiple time result of Ref. 7, we would consider our value for T_1 as an effective time. Our reported phase-memory time of 0.13 ± 0.05 ps is about ten times larger than the upper limit deduced from PS experiments.[4] This type of discrepancy between PS and RTOM experiments in relation to the phase-memory time has also been encountered in the case of the organic dye 1,3′ diethyl-2,2′ quinolylthia-carbocyanine iodide (DQCI).[10,11] In that case it turns out that spectral diffusion modifies the expected hole-burning linewidth of $2/T_2$ (HWHM) to give a larger linewidth. We think that we are in a similar situation here.

The largest value for the saturation parameter S was $S=0.13$, enough to cause saturation effects in the absorption of the pump beam. However, we did not observe this behavior.

Our analysis so far has been restricted to a two-band model, allowing for interband transitions and forbidding intraband transitions (related to spectral diffusion and orientational relaxation, for instance). Now, in picosecond recovery experiments in malachite green for low-viscosity solvents, only one relaxation time is observed.[12,13] At higher viscosities the relaxation time increases and, eventually, two relaxation times are observed. These observations entail the need to consider additional bands in the model. A simple two-band model is clearly not appropriate to describe experiments in all the range of viscosities. At low viscosity, however, the two-band model reproduces the RTOM spectra quite well and its simplicity and the capability to consider all orders of perturbation justifies its use. On the other hand, it is known that for the case of a three-band model the leading contribution to population oscillation (for malachite green) comes from the largest relaxation time.[4] Now, the fact that two- and three-band models yield predictions in agreement with experiments at low pump intensities, indicates that the additional relaxation times are short. However, one can expect that their contribution to population oscillations will become of importance at higher pumping intensities. This may be one source of disagreement between our two-band prediction of the broadening effect and the observed spectra at high intensity.

TABLE I. Population decay time of malachite green.

Population decay time (ps)	Solvent	Ref. no.
2	methanol	12
2±1	water	15
5±3	ethanol	16
2.8±1	methanol	13
1.2±0.1	water	4
0.78±1 and 7.4±3.0	water	7
from 0.34±0.04 to 7.3±3	water	7

Finally, intraband transitions have been shown to reduce the expected dc change of the population, as compared to transient's hole burning.[14,11] The influence of intraband transitions on the RTOM signal (for a two-band model in the third-order approximation) can be described by an effective two-band model, using the same transverse relaxation time and a longitudinal relaxation time that includes interband and intraband transitions.[2] The inclusion of intraband transitions and/or additional bands in our model may also give an explanation for the lack of saturation of the pump beam, and for any possible difference between the above two calculated transition moments. These facts are not accounted for a simple two-band model.

We conclude that saturation of the RTOM signal must be taken into account in the interpretation of the data, in order to determine the relaxation times. The modeling of malachite green with an effective two-level system with parameters $T_1=1.1\pm0.2$ ps, $T_2=0.13\pm0.05$ ps, and a transition moment of $1.2D$ accounts for the deviation from the third-order power dependence of the RTOM signal. For pump intensities below 10^8 W/cm^2, $S=0.06$, the broadening of the spectra can be predicted quite well, but for intensities of the order of 2×10^8 W/cm^2, departures from the predicted broadening can be observed. Also, previous perturbative calculations (up to fifth order) lead to the conclusion that power broadening always comes together with hole formation in a RTOM spectra. *We did not find such a hole, neither experimentally nor theoretically.* Now, considering that our calculations are at all order in the pump field and the only approximation is the scalar one, Eq. (13), we believe that such effect is artificially produced by the cutoff of the perturbation expansion. Finally, we mention that we have found similar saturation effects in a PS signal[17] which is expected from the above discussion.

ACKNOWLEDGMENTS

We wish to thank Professor R. Medina and Professor M. García Sucre for helpful discussions. This work was supported in part by Consejo Nacional de Investigaciones Cientificas y Tecnológicas (CONICIT), Caracas, Venezuela.

[1]T. Yajima, Opt. Commun. **14**, 378 (1975).
[2]T. Yajima and H. Souma, Phys. Rev. A **17**, 309 (1978).
[3]T. Yajima and H. Souma, Phys. Rev. A **17**, 324 (1978).
[4]J. J. Song, J. H. Lee, and M. D. Levenson, Phys. Rev. A **17**, 1439 (1978).
[5]J. H. Lee, J. J. Song, M. A. F. Scarparo, and M. D. Levenson, Opt. Lett. **5**, 196 (1980).
[6]A. E. Siegman, Appl. Phys. Lett. **30**, 21 (1977).
[7]Rick Trebino and A. E. Siegman, J. Chem. Phys. **79**, 3621 (1983).
[8]T. Yajima and Y. Taira, J. Phys. Soc. Jpn. **47**, 1620 (1979).
[9]A. Weiner and E. P. Ippen, Opt. Lett. **9**, 53 (1984).
[10]Y. Taira and T. Yajima, J. Phys. Soc. Jpn. **50**, 3459 (1981).
[11]F. García-Golding, J. Opt. Soc. Am. **73**, 59 (1983).
[12]E. P. Ippen, C. V. Shank, and A. Bergman, Chem. Phys. Lett. **38**, 611 (1976).
[13]V. Sundstrom *et al.*, Chem. Phys. **73**, 439 (1982).
[14]G. Mourou, IEEE J. Quantum Electron. **11**, 1 (1975).
[15]M. Stavola, G. Mourou, and W. Knox, Opt. Commun. **34**, 404 (1980).
[16]P. Wirth, S. Schneider, and F. Dörr, Opt. Commun. **20**, 155 (1977).
[17]A. Marcano O. and F. García-Golding, J. Chem. Phys. **82**, 1242 (1985).